Talanta 134 (2015) 271–277

Contents lists available at ScienceDirect

Talanta

journal homepage: www.elsevier.com/locate/talanta

Assembly-line manipulation of droplets in microfluidic platform for fluorescence encoding and simultaneous multiplexed DNA detection

Jinyang Chen, Guohua Zhou, Yufei Liu, Tai Ye, Xia Xiang, Xinghu Ji*, Zhike He*

Key Laboratory of Analytical Chemistry for Biology and Medicine (Ministry of Education), College of Chemistry and Molecular Sciences, Wuhan University, Wuhan 430072, P. R. China

ARTICLE INFO

Article history:
Received 10 September 2014
Received in revised form
11 November 2014
Accepted 13 November 2014
Available online 20 November 2014

Keywords:
Assembly-line manipulation
Microdroplet
Quantum dots
Encoding
Simultaneous detection

ABSTRACT

In this article, a new mode of droplets manipulation is presented and applied for simultaneous multiplexed DNA detection. We call this droplets manipulation, "assembly-line manipulation of droplets (ALMD)". Firstly, multiple droplets containing the same target mixtures are generated in the microchannel, and then fused with later generated different droplets containing corresponding probes, respectively. Finally, all the fused droplets were fluorescence imaged on-line and real-time. The successful implementation of droplets fluorescence encoding based on ALMD shows the reproducibility and accuracy of this manipulation mode. As a proof-of-concept application, the simultaneous multiplexed DNA detection was carried out through the model of human immunodeficiency virus (HIV) gene sequence and variola virus (small pox, VV) gene sequence based on ALMD in the microfluidic system. It is proved that this method achieves simultaneous multiplexed DNA measurements with a significantly time-saving way and without different dye-labelled probes or complex operation procedures. In addition, it reveals the possibility of high-throughput biosensing with simple chip design and detection equipment.

1. Introduction

The application of droplet platform in chemical and biological study has attracted increasing attention in recent years [1–5], such as material synthesis [6–8], cell analysis [9,10], protein detection [11–13], and DNA sensing [14,15]. Relative to the laminar flow-based microfluidics [16–18], droplet-based microfluidics possess many advantages, for instance, low reagent consumption, high mixing efficiency, short reaction time, and free of reagent immobilization, incubation, as well as cross-contamination. Therefore, as a promising tool, the droplet technique is in ceaseless development which is mainly in aspect of droplet manipulation and droplet application [19,20].

Analysis of DNA is of vital importance in diagnosing of genetic diseases, detection of gene expression profiling and biomedical studies [21–25]. Thanks to the potential capacity and advantage of droplet microfluidics, the interest of combining DNA sensing strategy with droplet platform is increasing recently. Consequently, droplet-based microfluidics has become one of the most popular platforms for DNA detection and analysis [26]. On one hand, as an isolated microreactor, the hybridization reaction of DNA in droplet is faster than that on conventional chips and without cross contamination of reagents. On the other hand, the droplet platform can perform affordable high-throughput assay with low reagent consumption and short time. A variety of researches such as DNA detection and mutant analysis [27,28], as well as DNA sequencing [29] have been carried out in droplet-based microfluidic systems. However, these applications were confined in single-analyte assays because of identical droplet detection. In addition, due to the difficulty of droplets control, the detection process usually requires expensive instruments to realize, which limits the application scope of droplet platform. With the development of manipulation technologies, such as transportation, fusion, trapping, and storage [30–32], a manipulated droplet platform was proposed for the detection of DNA. For the purpose of multiplexed measurements, based on fluorescence resonance energy transfer (FRET) between fluorescent dye and graphene oxide, a simultaneous colorimetric method for two different DNA sequences was realized by analyzing the fluorescence variation of different fluorescent dyes in droplets [33]. In this way, when the number of analytes is up to three or more, more DNA probes labeled with different dyes which can be distinguished directly by colorimetry will be needed. Furthermore, a new droplet platform based on stepwise reagent introduction has been applied in multiplexed DNA sensing meets the challenge of multi-targets analysis without different dyes-labelled probes [34]. Never the less, the above methods were achieved in a mode of single droplet

* Corresponding authors. Tel.: +86 27 68756557; fax: +86 27 68754067.
E-mail address: zhkhe@whu.edu.cn (Z. He).

http://dx.doi.org/10.1016/j.talanta.2014.11.027
0039-9140/

manipulation and imaging in one time. It means that the experiment will last for a long time if there are many analytes, accompanying with relative large experimental errors which will be existed in different droplets detection. What's more, it's not favourable for the developing trend of high-throughput analysis.

Inspired by the mentioned above, herein, we present a microfluidic platform that combines assembly-line manipulation of droplets (ALMD) with multi-droplets concurrently imaging to detect multiplex DNAs. This droplet platform addresses the challenge of multi-analytes analysis, such as simplicity, low cost and time-saving, which is ideal in high-throughput format. The solutions of DNA targets, two corresponding DNA probes labeled with carboxytetramethylrhodamine (TAMRA) and graphene oxide are individually imported into the side channels. After ALMD, two captured droplets are imaging in one photograph. By comparing and analyzing the variation of droplet color and fluorescence intensity, the qualitative and quantitative measurements of target DNAs are realized.

2. Experimental

2.1. Materials

Graphene oxide (GO) was purchased from Sinocarbon Materials Technology Co., Ltd. Mineral oil and Span 80 were purchased from Sigma-Aldrich. Water-soluble Zn^{2+} doped CdTe quantum dots (QDs) were synthesized according to references [35]. The silicon wafer was purchased from Institute of Microelectronics of Chinese Academy of Sciences. The poly-(dimethylsiloxane) (PDMS) and AZ 50 XT photoresist was obtained from RTV615 GE Toshiba Silicones Co., Ltd. and AZ Electronic Materials USA Corp., respectively. DNA oligonucleotides were synthesized and purified by Sangon Biotechnology Co., Ltd. (Shanghai, China). The sequences of the oligonucleotides were as follows:

DNA probe for VV sequence (P_{VV}): 5′–TAMRA-CTGATTACTATTGCATCTTCCGTTACAACTATCAG-3′;
DNA probe for HIV sequence (P_{HIV}): 5′–TAMRA-TGCATCCAGGTCATGTTATTCCAAATATCTTCTATGCA-3′;
target sequence of VV (T_{VV}): 5′–AGTTGTAACGGAAGATGCAATAGTAATCAG-3′;
target sequence of HIV (T_{HIV}): 5′–AGAAGATATTTGGAATAACATGACCTGGATGCA-3′;
single-base mismatched target DNA of VV (MT_{VV}): 5′–AGTTGTAACGGAA*T*ATGCAATAGTAATCAG-3′;
single-base mismatched target DNA of HIV (MT_{HIV}): 5′- AGAAGATATTTGGAATAA*T*ATGACCTGGATGCA-3′

The DNA solution was prepared in 10 mM Tris–HCl buffer (20 mM NaCl and 20 mM $MgCl_2$, pH 7.4). Other aqueous solutions were prepared with ultrapure water (Mill-Q, Millipore, 18.2 MΩ · cm, 25 °C).

2.2. Microfluidic chip fabrication and operation

The three-layer PDMS microfluidic chip was fabricated by soft-photolithography. The bottom, middle, and upper is glass, automatic microvalve and fluid layer, respectively. Details of fabrication are explained in Supplementary Information. There were four T-junction structures and several microvalves in this chip. The main and injection channels are 200 μm wide and the valve channels are 100 μm. The microvalves were pneumatically actuated by a homemade pressure control system (SeriesZSE30A (F)/ISE30A, SMC, Japan, shown in Fig. S1) which was connected to a personal computer (PC). So the on/off state of the microvalves could be controlled through PC. The syringe pumps (11 plus, Harvard Apparatus Holliston, USA) were used to pump the oil phase (containing 0.1% Span 80) into the channels. The aqueous solutions were loaded into a section of flexible polyethylene tubing, and then were driven into the microchannels by the positive pressure supplied by pressure control system.

2.3. Procedure for multiplexed DNA sensing based on ALMD

By controlling the microvalves, droplets generation, transportation, fusion and trapping could be realized. The details were described previously [36]. The main channel was used for oil introduction and the side ones were used for the introduction of target mixtures, P_{VV}, P_{HIV}, and GO, respectively. For ALMD, the pair of uniform-sized droplets of target mixtures was generated firstly. Under the driving force of oil phase, these two droplets were transported to the next side channel junction and the front droplet was fused with droplet of P_{VV}. Next, the latter droplet was fused with droplet of P_{HIV} when it arrived at the third junction. Finally,

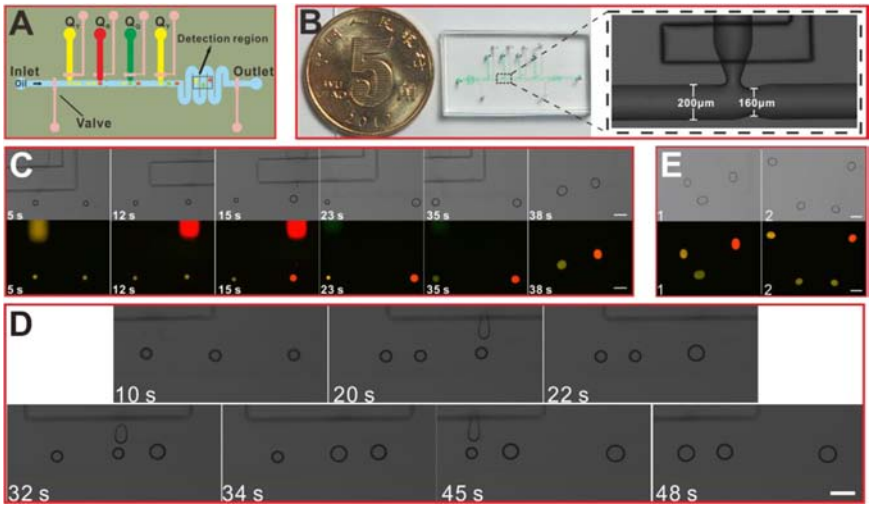

Fig. 1. (A) Schematic diagram of the structure of droplet chip and the procedure of ALMD. (B) Photograph of the microfluidic chip and bright field image of bottleneck design within the main channel. (C) Procedure of assembly-line manipulation of two droplets through the model of different QDs. (D) Procedure of three droplets manipulation in assembly-line pattern. (E) Simultaneously capturing and imaging multi-droplets after the assembly-line manipulation: (1) three droplets; (2) four droplets. Above: bright field images; below: corresponding fluorescence images. Scale bars indicate 200 μm.

these two droplets were fused with GO droplet successively and respectively in the last junction. And these droplets were trapped in the detection region to take a true-color fluorescence image for DNA assay. In the same manner, droplets fluorescence encoding based on ALMD was carried out. All droplets were imaged by an inverted fluorescence microscope (Axio Observer.A1, Zeiss, Germany) with a 10× objective and a Spot RT3 charge-coupled device (CCD, Diagnostic Instruments, Inc., USA). The fluorescence intensity of droplet was acquired by Image-Pro Plus software.

3. Results and discussions

3.1. Feasibility of ALMD

In order to meet the challenge of high-throughput biosensing, the strategy of high-throughput droplets generation should be proposed. Herein, the microfluidic platform based on ALMD can be the candidate for high-throughput analytical platform. The structure diagram of chip and the scheme of droplets manipulation are shown in Fig. 1A. On the basis of classical T-junction channel, a bottleneck design was introduced next to the side channel junction with the purpose of easy manipulation of droplets in assembly-line pattern. The photographs of the microfluidic chip (22 mm × 12 mm × 4 mm) and the bottleneck design within the main channel are presented in Fig. 1B. The main and side channels were 200 μm wide and the bottlenecks were 160 μm wide. It is worth to note that bottleneck design within the main channel is favorable for the droplets trapping and fusion, because the droplets will have a slight pause when they arrive at the side channel junction. Moreover, in order to address the issue of the small observation field of microscope, which limits the concurrently imaging of multi-droplets, the detection region was designed to be serpentine channel. In this way, droplets can be crowded in the square observation field, so that several droplets can be imaged simultaneously within one detection field. As a model, different QDs (λ_{em}=535 nm; 578 nm; 648 nm) were introduced into the three chip channels, respectively. The 578 nm QD (Q_Y), 648 nm QD (Q_R) and 535 nm QD (Q_G) were individually imported into the side channels. By controlling the valves, two droplets containing Q_Y were generated successively, and then fused with Q_R and Q_G droplets, respectively. The bright-field and fluorescence images in Fig. 1C clearly display the processes of the two droplets manipulation in assembly-line pattern. Moreover, when we introduced four solutions of Q_Y, Q_R, Q_G, and Q_Y into four side channels, respectively, we can obtain three droplets of Q_Y fused with Q_R, Q_G and Q_Y, respectively. The whole procedure from droplets generation to imaging for analysis could be accomplished within 1 min (Fig. 1D). As shown in the fluorescence image (Fig. 1E1), three droplets were captured in one picture, and the true colors of them revealed the successful fusion of droplets as expected. In the same mode, four droplets can be manipulated in assembly-line pattern and imaged as well (Fig. 1E2). Therefore, it is proved that ALMD can be easily and rapidly realized with the simple micro-chip.

3.2. Droplets fluorescence encoding

By controlling the loading pressure of the aqueous solution and the open time of the valves, the manipulation of droplets could be carried out very precisely [36]. We tested this precise manipulation and applied it in droplets fluorescence encoding. As a proof-of-concept demonstration, three solutions of buffer, Q_R and Q_G were chosen for fluorescence encoding. Since the concentrations of QDs in droplets after fusion were determined by the volume ratio of two original droplets, the desired fluorescence intensities and colors of droplets could be obtained by varying the volume ratios of original droplets individually during the process of droplets manipulation. Firstly, we manipulated multi-droplets in assembly-line pattern allowing droplets to fuse with each other once, so that we obtained three fusions of droplets. As shown in Fig. 2A, the fluorescence intensity ratios of Q_R and Q_G in final droplets to original droplets were equal to the volume ratios of corresponding original droplets to final droplets. For relative complicated droplets fluorescence encoding, we allowed each droplet to fuse with both of two others. Hence each droplet contained all of the three solutions in variable volume ratios. The results showed that experimental variation in fluorescence intensities of the droplets has good agreements with the volume ratios between the three solutions as well (Fig. 2B). Therefore, it is proved the ALMD could be controlled precisely with good

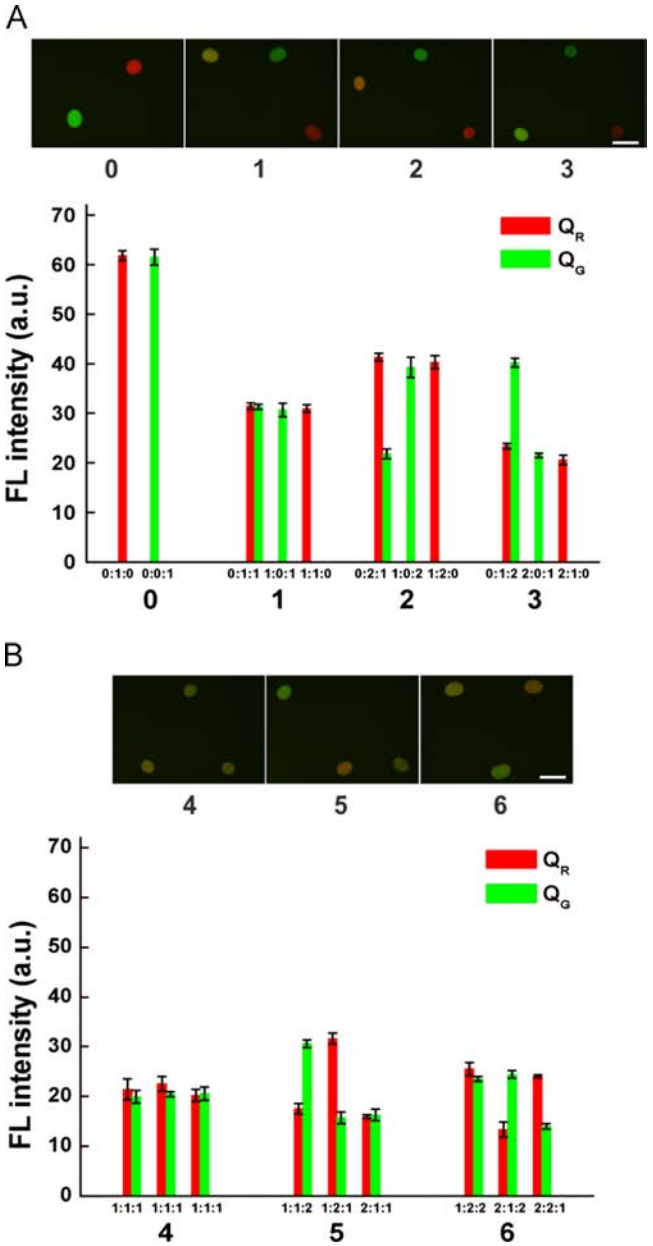

Fig. 2. Droplets fluorescence encoding based on ALMD. (A) Allowing each droplet to be fused only once ((A0) shows the initial concentration of Q_R and Q_G). The volume ratios of buffer droplet/Q_R droplet/Q_G droplet were (1) 0:1:1, 1:0:1, 1:1:0; (2) 0:2:1, 1:0:2, 1:2:0; (3) 0:1:2, 2:0:1, 2:1:0. (B) Allowing each droplet to be fused twice. The volume ratio s of buffer droplet/Q_R droplet/Q_G droplet were (4) 1:1:1, 1:1:1, 1:1:1; (5) 1:1:2, 1:2:1, 2:1:1; (6) 1:2:2, 2:1:2, 2:2:1. The corresponding fluorescence intensities of two QDs in each droplet were presented below. Scale bars indicate 300 μm.

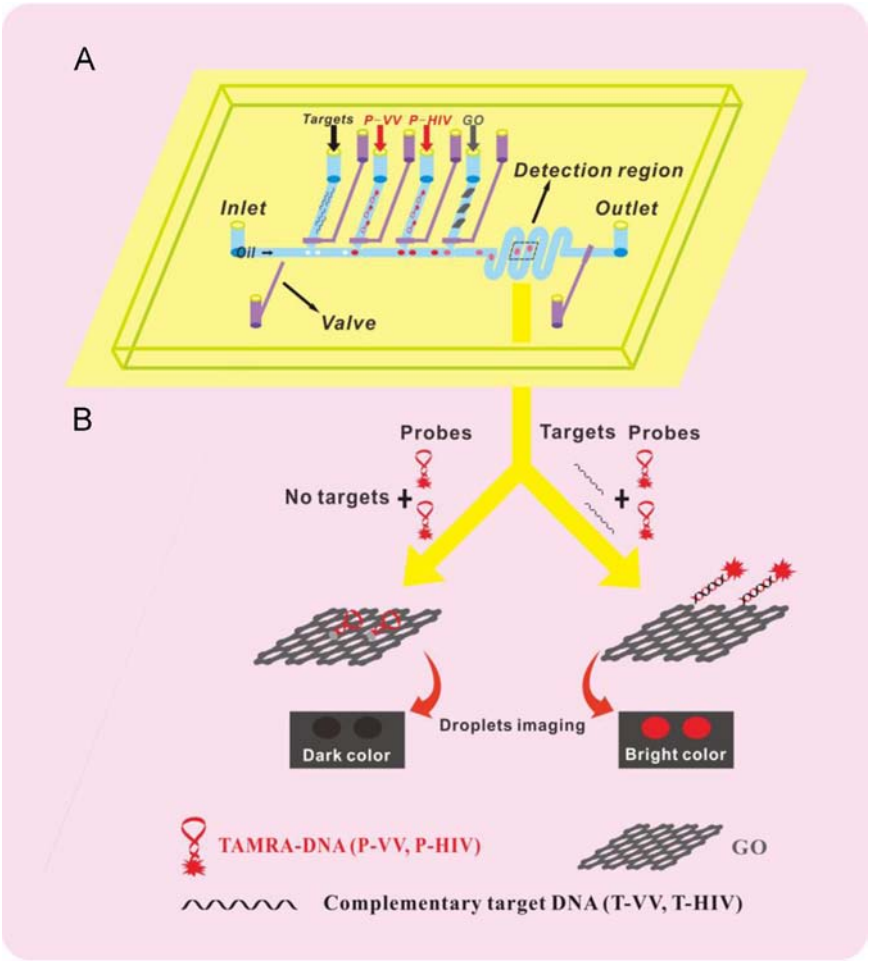

Fig. 3. (A) Schematic diagram of the procedures of simultaneous multiplexed DNA sensing based on ALMD. (B) Schematic illustration of the principle of multiplexed DNA sensing.

reproducibility, and suited for the application of low cost, time-saving fluorescence encoding of droplets.

3.3. Multiplexed DNA sensing strategy

Since fluorescence quenching strategies have been widely applied in biosensing, a variety of fluorescence quenching materials, such as conducting polymers [37], gold nanoparticles [38], carbon nanotubes [39], are used in biosensor design. More recently, GO-based biosensor has attracted a lot of research interests [40–42]. It has been reported that these biosensors are based-on the capability to discriminate single-stranded DNA (ssDNA) and double-stranded DNA (dsDNA) coupled with the extraordinary fluorescence quenching of GO [43]. Taking advantages of this GO-based biosensor, multiplexed DNA sensing could be realized based on ALMD. The schematic illustration of the droplets manipulation and principle of detection are shown in Fig. 3. In the absence of T_{VV} and T_{HIV}, TAMRA-modified P_{VV} and P_{HIV} were absorbed on the surface of GO, and the fluorescence of TAMRA-labelled probes were quenched by GO. Consequently, both of the two droplets were presented in dark color (Fig. S2A). In the presence of T_{HIV}, it induced the formation of dsDNA by the hybridization with P_{HIV}. As a result, a fluorescent emission was observed due to the weaker interaction between the formed duplex helix and GO. As shown in the image, only the droplet with P_{HIV} displayed red color, while the other one containing P_{VV} was presented in dark color (Fig. S2B). According to the same principle, in the presence of T_{VV}, the droplet containing P_{VV} was presented in red color while the other one was presented in dark color (Fig. S2C). When the target DNA mixtures containing both of T_{HIV} and T_{VV}, two red droplets appeared in the fluorescence image as expected (Fig. S2D). Therefore, simultaneously multiplexed DNA analysis can be performed by this manipulation of droplets in assembly-line pattern, with the feature of simple and straightforward, as well as time-saving.

3.4. Optimization of the amount of GO

In order to obtain obvious droplet color changes, the volume ratio between probe and GO droplet was investigated. The concentrations of DNA probe was fixed at 4×10^{-5} M for the purpose of acquiring strong fluorescence signal. Owing to the adsorption of GO on PDMS, the droplet with high GO concentration was hard to form. The concentration of GO was thus fixed at 0.4 mg/mL. As shown in Fig. 4A and a, the fluorescence signal of the final droplet containing P_{VV} and GO was reduced with the increase of the volume ratio of P_{VV} droplet to GO droplet from 1:1 to 1:4. Though the fluorescence of TAMRA-modified P_{VV} was quenched totally when the volume ratio was 1:4, the concentration of P_{VV} was further diluted with the addition of target droplet, leading to the bad fluorescence recovery, which should be unfavorable for the detection sensitivity. Moreover, by fixing the T_{VV} droplet size as the same as P_{VV} droplet, we discussed the fluorescence recovery corresponding to different volume ratios of P_{VV} to GO droplet. As illustrated in Fig. 4B, the droplet color became weaker and weaker with the volume ratio of probe/target/GO droplets changed from 1:1:1 to 1:1:4. By comparing the droplet color variation in the absence and presence of T_{VV} under different volume ratios of probe to GO, the change of droplet color was the greatest at the ratio

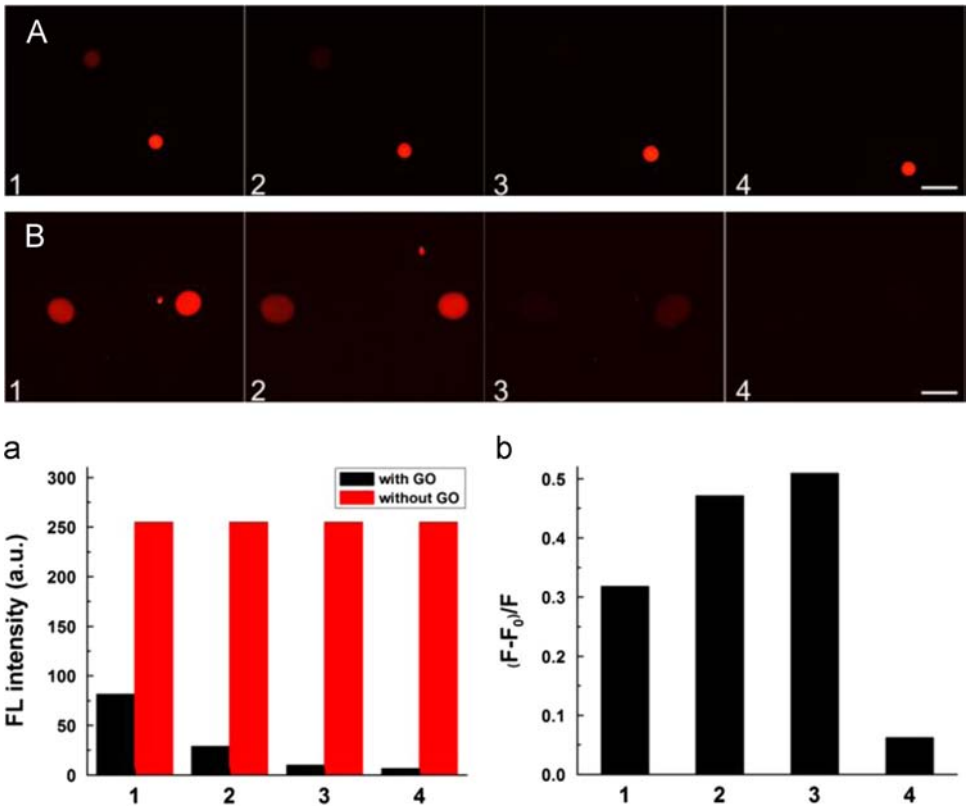

Fig. 4. (A) Color responses of two droplets of P_{VV} in the presence (left droplet) and absence (right droplet) of GO. The volume ratios of P_{VV} to GO droplet were 1:1, 1:2, 1:3, and 1:4 from 1 to 4. (B) Color responses of two droplets of P_{VV}-GO in the absence (left droplet) and presence (right droplet) of T_{VV}. The volume ratios of P_{VV}/T_{VV}/GO droplet were 1:1:1, 1:1:2, 1:1:3, and 1:1:4 from 1 to 4. The corresponding fluorescence intensities of (A) were presented in (a). (b) Color variation of the two droplets within each picture from B1 to B4. F and F_0 are the fluorescence intensity of droplet in the presence and absence of T_{VV}. The initial concentrations of T_{VV}, P_{VV}, and GO were 5.0×10^{-7} M, 4.0×10^{-5} M and 0.4 mg/mL, respectively. Scale bars indicate 200 μm.

of 1:3 (Fig. 4b). Consequently, the volume ratio of probe/target/GO droplets was chosen as 1:1:3.

3.5. Sensitivity for simultaneously multiplexed DNA detection

To further evaluate the sensitivity of this method, various concentrations of target DNAs were introduced into the sensing ensemble. Under optimized conditions, the simultaneous detection of T_{HIV} and T_{VV} was carried out. As shown in Fig. 5, with the change of concentrations of target DNAs, a series of color variation of droplets was presented. The light red color appeared firstly, and then gradually turned brighter and brighter, which indicated that the more dsDNA formed with the increase of target, leading to DNA probe being away from the surface of GO and the fluorescence recovery of TAMRA. Therefore, the targets could be determined qualitatively and quantitatively by the color or the fluorescence intensity of droplets. It is found that the fluorescence intensities of droplets were linearly related to the logarithm of targets concentrations over the range from 2.5×10^{-8} to 5.0×10^{-6} M. The limit of detection for T_{HIV} and T_{VV} were calculated as 1.4×10^{-8} and 1.6×10^{-8} M, respectively, based on a linear fitting and the noise level of 3σ (where σ is the standard deviation of a blank solution, $n=11$).

3.6. Specificity of DNA sensing

Generally, non-specific binding often results in high background and low sensitivity. Thus we evaluated the specificity of DNA sensing by this method. In the presence of complementary target DNAs (Ts), the fused droplets were shown in bright red color according to the fluorescence images (Fig. 6A). In control experiments with the presence of single-base mismatched target DNAs (MTs), the droplets were presented in light colors (Fig. 6B). The background signal was detected in the absence of MTs or Ts under the same experimental conditions. The results suggested that the fluorescence signals of probes-GO droplets for MTs were significantly lower than that for Ts, because of the weak hybridization between MTs and DNA probes resulting from the tension in the stem-loop structure of probes. Therefore, this simultaneous detection strategy can realize DNA differentiation with good selectivity.

3.7. Determination of target DNAs in complex matrix

In order to evaluate the practicability of the proposed method in multiplexed DNA assay, the detection of target DNA mixtures in human serum was investigated. As the human serum with high concentration has a significant effect on the generation and fusion of droplets in microfluidic system, the proposed strategy could be applied in the complex matrix with a high serum percentage by diluting the complex matrix. Dilution to 1% was chosen in this work. Three kind of different concentrations of target DNA mixtures were detected in buffer and 1% human serum, respectively, the results were shown in Fig. S3. The fluorescence intensities of final droplets in the conditions of diluted human serum have no significant difference with those in buffer. It indicates that the complex matrix has no obvious influence on multiplexed DNA assay based on ALMD.

4. Conclusions

In conclusion, a new droplets manipulation mode, ALMD is presented. This method is easily achieved without complicated operation and expensive instruments. By precisely controlling of droplets

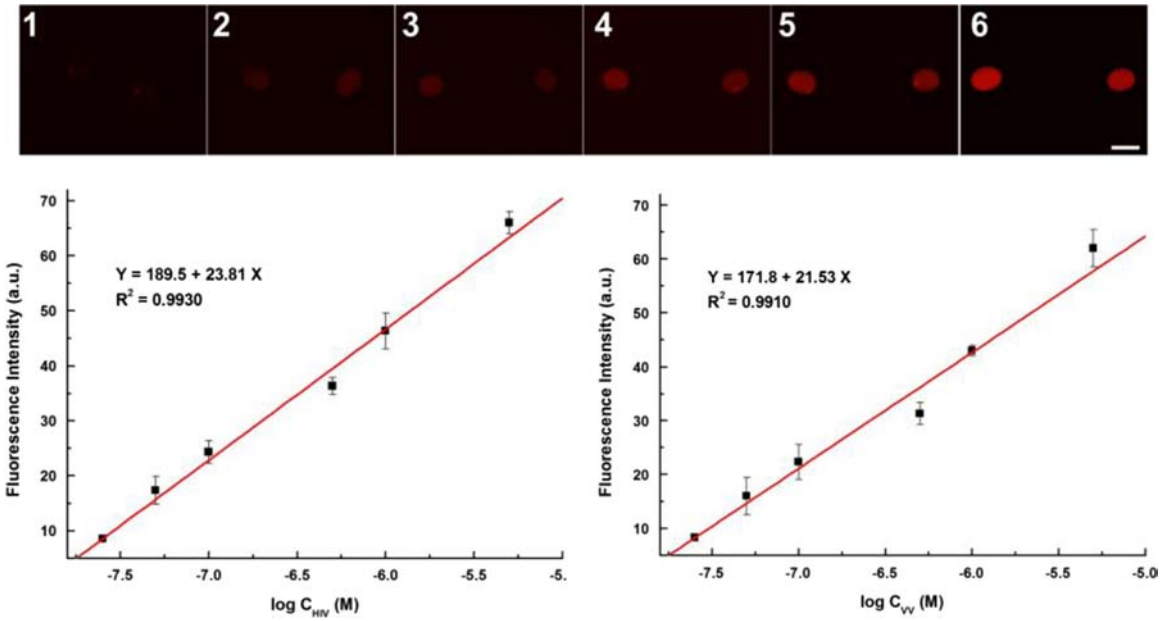

Fig. 5. Color responses of two droplets of probe-GO in the coexistence of T_{HIV} (left droplet) and T_{VV} (right droplet) with increasing concentrations of 2.5×10^{-8}, 5.0×10^{-8}, 1.0×10^{-7}, 5.0×10^{-7}, 1.0×10^{-6}, 5.0×10^{-6} M from 1 to 6. The following diagram presented the relationships between the fluorescence intensities and the concentrations of corresponding target DNAs. The volume ratios of DNA probe/target DNAs/GO were 1:1:3. Other experimental conditions were the same as in Fig. 4. Scale bar indicates 200 μm.

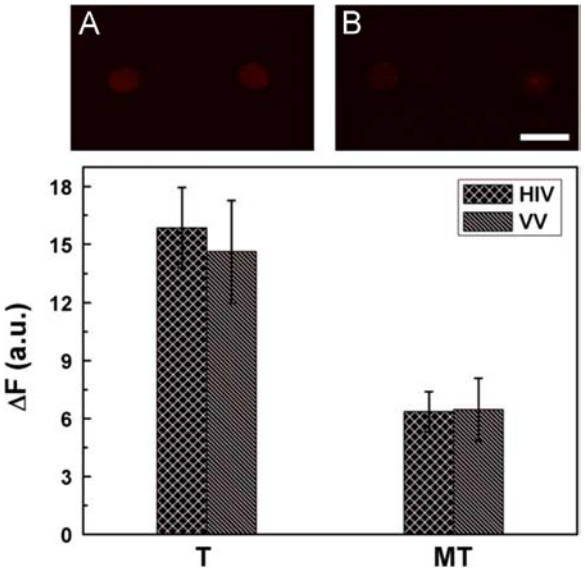

Fig. 6. Color responses of two droplets of probe-GO in the presence of Ts (A) and MTs (B). The corresponding fluorescence intensities were presented below. The initial concentrations of Ts and MTs were 5.0×10^{-7} M. The volume ratios of DNA probe/target DNAs/GO were 1:1:3. Other experimental conditions were the same as in Fig. 4. Scale bar indicates 200 μm.

generation and fusion, fluorescence encoding of droplets can be carried out with ALMD in microfluidic platform. Besides, the manipulation of droplets in assembly-line pattern is very suitable for simultaneously on-line detection of multiplex DNAs in micro-chip. Therefore, it has been successfully applied in simultaneously multiplexed DNA sensing through the model of HIV and VV gene sequence. It is indicated that more targets could be simultaneously detected based on ALMD with the increase of more probe introduction microchannels in chip. So the low cost and significantly time-saving droplet platform shows the potential in simultaneously high-throughput DNA assay.

Acknowledgments

This work was supported by the National Key Scientific Program-Nanoscience and Nanotechnology (2011CB933600) and the National Science Foundation of China (21275109, 21205089).

Appendix A. Supporting information

Supplementary data associated with this article can be found in the online version at http://dx.doi.org/10.1016/j.talanta.2014.11.027.

Reference

[1] A.B. Theberge, F. Courtois, Y. Schaerli, M. Fischlechner, C. Abell, F. Hollfelder, W.T. Huck, Angew. Chem., Int. Ed. 49 (2010) 5846–5868.
[2] X. Casadevall i Solvas, A. deMello, Chem. Commun. 47 (2011) 1936–1942.
[3] M.T. Guo, A. Rotem, J.A. Heyman, D.A. Weitz, Lab Chip 12 (2012) 2146–2155.
[4] H.N. Joensson, H. Andersson Svahn, Angew. Chem., Int. Ed. 51 (2012) 12176–12192.
[5] C.H. Chiou, D.J. Shin, Y. Zhang, T.H. Wang, Biosens. Bioelectron. 50 (2013) 91–99.
[6] S. Duraiswamy, S.A. Khan, Small 5 (2009) 2828–2834.
[7] J.H. Kim, T.Y. Jeon, T.M. Choi, T.S. Shim, S.-H. Kim, S.-M. Yang, Langmuir 30 (2013) 1473–1488.
[8] J.T. Wang, J. Wang, J.J. Han, Small 7 (2011) 1728–1754.
[9] S.Q. Gu, Y.X. Zhang, Y. Zhu, W.B. Du, B. Yao, Q. Fang, Anal. Chem. 83 (2011) 7570–7576.
[10] S. Cho, D.K. Kang, S. Sim, F. Geier, J.Y. Kim, X. Niu, J.B. Edel, S.I. Chang, R.C. Wootton, K.S. Elvira, A.J. deMello, Anal. Chem. 85 (2013) 8866–8872.
[11] J.W. Choi, D.K. Kang, H. Park, A.J. deMello, S.I. Chang, Anal. Chem. 84 (2012) 3849–3854.
[12] L.F. Cai, Y. Zhu, G.S. Du, Q. Fang, Anal. Chem. 84 (2012) 446–452.
[13] Z. Han, W. Li, Y. Huang, B. Zheng, Anal. Chem. 81 (2009) 5840–5845.
[14] M. Srisa-Art, A.J. deMello, J.B. Edel, Chem. Commun. (2009) 6548–6550.
[15] F. Guo, M.I. Lapsley, A.A. Nawaz, Y. Zhao, S.C. Lin, Y. Chen, S. Yang, X.Z. Zhao, T.J. Huang, Anal. Chem. 84 (2012) 10745–10749.
[16] M. Meier, E.M. Lucchetta, R.F. Ismagilov, Lab Chip 10 (2010) 2147–2153.
[17] M. Vojtisek, A. Iles, N. Pamme, Biosens. Bioelectron. 25 (2010) 2172–2176.
[18] Y. Gao, L. Chen, Lab Chip 8 (2008) 1695–1699.
[19] T. Schneider, J. Kreutz, D.T. Chiu, Anal. Chem. 85 (2013) 3476–3482.
[20] K. Zhang, Q. Liang, X. Ai, P. Hu, Y. Wang, G. Luo, Anal. Chem. 83 (2011) 8029–8034.
[21] R.M. Kong, Z.L. Song, H.M. Meng, X.B. Zhang, G.L. Shen, R.Q. Yu, Biosens. Bioelectron. 54 (2014) 442–447.

[22] M. Luo, N. Li, Y. Liu, C. Chen, X. Xiang, X. Ji, Z. He, Biosens. Bioelectron. 55 (2014) 318–323.
[23] J. Thavanathan, N.M. Huang, K.L. Thong, Biosens. Bioelectron. 55 (2014) 91–98.
[24] Y. Zhao, F. Chen, M. Lin, C. Fan, Biosens. Bioelectron. 54 (2014) 565–570.
[25] W. Zhou, X. Gong, Y. Xiang, R. Yuan, Y. Chai, Biosens. Bioelectron. 55 (2014) 220–224.
[26] L. Mazutis, A.F. Araghi, O.J. Miller, J.C. Baret, L. Frenz, A. Janoshazi, V. Taly, B.J. Miller, J.B. Hutchison, D. Link, A.D. Griffiths, M. Ryckelynck, Anal. Chem. 81 (2009) 4813–4821.
[27] A.T.H. Hsieh, P.J.H. Pan, A.P. Lee, Microfluid. Nanofluid. 6 (2009) 391–401.
[28] D. Pekin, Y. Skhiri, J.C. Baret, D. Le Corre, L. Mazutis, C.B. Salem, F. Millot, A. El Harrak, J.B. Hutchison, J.W. Larson, D.R. Link, P. Laurent-Puig, A. D. Griffiths, V. Taly, Lab Chip 11 (2011) 2156–2166.
[29] A.R. Abate, T. Hung, R.A. Sperling, P. Mary, A. Rotem, J.J. Agresti, M.A. Weiner, D.A. Weitz, Lab Chip 13 (2013) 4864–4869.
[30] H. Boukellal, S. Selimovic, Y. Jia, G. Cristobal, S. Fraden, Lab Chip 9 (2009) 331–338.
[31] D.R. Link, E. Grasland-Mongrain, A. Duri, F. Sarrazin, Z. Cheng, G. Cristobal, M. Marquez, D.A. Weitz, Angew. Chem., Int. Ed. 45 (2006) 2556–2560.
[32] X. Niu, S. Gulati, J.B. Edel, A.J. deMello, Lab Chip 8 (2008) 1837–1841.
[33] X. Xiang, M. Luo, L. Shi, X. Ji, Z. He, Anal. Chim. Acta 751 (2012) 155–160.
[34] X. Xiang, L. Shi, M. Luo, J. Chen, X. Ji, Z. He, Biosens. Bioelectron. 49 (2013) 403–409.
[35] D. Zhao, Y. Fang, H. Wang, Z. He, J. Mater. Chem. 21 (2011) 13365.
[36] X. Xiang, L. Chen, Q. Zhuang, X. Ji, Z. He, Biosens. Bioelectron. 32 (2012) 43–49.
[37] A. Ramanavicius, N. Ryskevic, Y. Oztekin, A. Kausaite-Minkstimiene, S. Jursenas, J. Baniukevic, J. Kirlyte, U. Bubniene, A. Ramanaviciene, Anal. Bioanal. Chem. 398 (2010) 3105–3113.
[38] D.J. Maxwell, J.R. Taylor, S.M. Nie, J. Am. Chem. Soc. 124 (2002) 9606–9612.
[39] R.H. Yang, J.Y. Jin, Y. Chen, N. Shao, H.Z. Kang, Z. Xiao, Z.W. Tang, Y.R. Wu, Z. Zhu, W.H. Tan, J. Am. Chem. Soc. 130 (2008) 8351–8358.
[40] K. Hu, J. Liu, J. Chen, Y. Huang, S. Zhao, J. Tian, G. Zhang, Biosens. Bioelectron. 42 (2013) 598–602.
[41] T. Kuila, S. Bose, P. Khanra, A.K. Mishra, N.H. Kim, J.H. Lee, Biosens. Bioelectron. 26 (2011) 4637–4648.
[42] C.H. Lu, H.H. Yang, C.L. Zhu, X. Chen, G.N. Chen, Angew. Chem., Int. Ed. 48 (2009) 4785–4787.
[43] S. He, B. Song, D. Li, C. Zhu, W. Qi, Y. Wen, L. Wang, S. Song, H. Fang, C. Fan, Adv. Funct. Mater. 20 (2010) 453–459.